



Quantifying fluxes and characterizing compositional changes of dissolved organic matter in aquatic systems in situ using combined acoustic and optical measurements

Journal:	<i>Limnology and Oceanography: Methods</i>
Manuscript ID:	draft
Manuscript Category:	New Methods
Date Submitted by the Author:	n/a
Complete List of Authors:	Downing, Bryan; U.S.Geological Survey, CA Water Science Center
Keywords:	optical, DOM, DOC, in situ, tidal wetlands



Only

1
2
3 1 **Quantifying fluxes and characterizing compositional changes of dissolved organic matter in**
4
5 2 **aquatic systems *in situ* using combined acoustic and optical measurements**
6
7
8 3

9
10 4 Bryan D. Downing,¹ Emmanuel Boss,² Brian A. Bergamaschi,¹ Jacob A. Fleck,¹ Megan A.
11
12 5 Lionberger,¹ Neil K. Ganju,¹ David H. Schoellhamer,¹ and Roger Fujii¹
13
14 6

15
16
17 7 ¹ *Water Science Center, US Geological Survey, Sacramento, CA, USA.*

18
19 8 ² *School of Marine Sciences, University of Maine, Orono, ME, USA.*
20
21 9

22
23
24 10 ***Abstract***

25
26
27 11 Studying the dynamics and geochemical behavior of dissolved and particulate organic material
28
29 12 is difficult because the concentration and composition may rapidly change in response to
30
31 13 aperiodic as well as periodic physical and biological forcing. Here we describe a method useful
32
33 14 for quantifying fluxes and analyzing dissolved organic matter (DOM) dynamics. The method
34
35 15 uses coupled optical and acoustic measurements that provide robust quantitative estimates of
36
37 16 concentrations and constituent characteristics needed to investigate processes and calculate
38
39 17 fluxes of DOM in tidal and other lotic environments. Data were collected several times per hour
40
41 18 for two weeks or more, with the frequency and duration limited only by power consumption and
42
43 19 data storage capacity. The capabilities and limitations of the method are assessed using data
44
45 20 from a winter deployment in a natural tidal wetland of the San Francisco Bay estuary. Statistical
46
47 21 correlation of *in situ* optical data with traditional laboratory analyses of discrete water samples
48
49 22 was used to calibrate optical properties suited as proxies for DOM concentrations and
50
51 23 characterizations. Coupled with measurements of flow velocity calculation of long term residual
52
53
54
55
56
57
58
59
60

1
2
3 24 horizontal fluxes of DOC into and out from a tidal wetland are obtained. Subsampling the dataset
4
5 25 provides an estimate for the maximum sampling interval beyond which the error in flux estimate
6
7
8 26 is significantly increased.
9
10
11 27

12
13 28 *Keywords: Optical, DOM, DOC, in situ, tidal wetlands.*
14
15 29

16
17 30 *Running head: In situ measurements for DOC fluxes and characterization*
18
19
20
21
22
23
24
25
26
27
28
29
30
31
32
33
34
35
36
37
38
39
40
41
42
43
44
45
46
47
48
49
50
51
52
53
54
55
56
57
58
59
60

1
2
3 31 ***Introduction***
4

5 32 It is well established that dissolved organic matter (DOM) plays a major role in
6
7
8 33 biogeochemical processes: it supplies energy to heterotrophic organisms, binds metals and
9
10 34 pesticides, affects light penetration, influences particle aggregation, and interaction of biota with
11
12 35 synthetic organic compounds and trace metals (e.g. Mantoura et al., 1978, Aiken et al., 1985).
13
14
15 36 However, the full ecological significance of DOM has not been fully elucidated, in part because
16
17 37 of the difficulties involved in quantifying changes in concentration, source, composition, and
18
19
20 38 bioavailability at timescales appropriate to physical forcings such as tides and storms. This study
21
22 39 examines the efficacy of using a combination of *in situ* optical and acoustic measurements to
23
24 40 quantify fluxes and examine changes in chemical properties of DOM in a tidal wetland system,
25
26
27 41 but the results could be of use for studies in many lotic environments.
28

29 42 Optical properties measured in natural waters are used as proxies to concentration of
30
31 43 biogeochemical parameters such as nitrate, sulfide, dissolved organic carbon (DOC), particulate
32
33 44 organic material, chlorophyll, and others (e.g. Johnson et al., 2006, Boss et al., 2007, Claustre et
34
35 45 al., 2008). Recently developed, commercially available instrumentation provide the ability to
36
37 46 measure optical properties *in situ*, potentially permitting nearly continuous assessment of the
38
39 47 concentration of some important biogeochemical parameters. For example, the deployment of an
40
41 48 in-situ spectrophotometer with 0.2 μ m pre-filters provides the opportunity to measure the
42
43 49 absorption properties of DOM and its spectral behavior (Twardowski et al., 1999).
44
45

46 50 Therefore, *in situ* deployment of optical instrumentation may permit the collection of
47
48 51 biogeochemical data on temporal and spatial scales needed to resolve episodic, rapid, and short-
49
50 52 timescale environmental forcing (time scales of tens of minutes)—an undertaking that is
51
52 53 impractical with conventional discrete sampling and laboratory analysis (Dickey, 2001). For
53
54
55
56
57
58
59
60

1
2
3 54 example, Johnson et al. (2006) has demonstrated the utility of high frequency *in situ* absorption
4
5 55 measurements for determination of nitrate concentrations and their dynamics in an estuary. We
6
7
8 56 describe below the relationship between optical parameter values and laboratory measurements
9
10 57 of DOC concentration, and use this relationship to obtain a multi-week high-resolution record of
11
12 58 DOC concentration from in-situ optical data. In principle, a similar technique could be used for
13
14 59 other biogeochemical parameters having an optical proxy. We do not propose that *in situ* optical
15
16 60 parameter measurements replace conventional discrete sampling, but rather be used to interpolate
17
18 61 between or extrapolate beyond the discrete samples.
19
20

21
22 62 Importantly, for DOM, simultaneous measurement of spectral absorption and DOM
23
24 63 fluorescence provides an opportunity to characterize DOM in terms of its absorption spectral
25
26 64 slope and the ratio of fluorescence to absorption parameters related to the chemical composition
27
28 65 of DOM (Carder et al. 1989, Blough and Green 1995, Yacobi et al., 2003).
29
30

31
32 66 Previous studies have used optical measurements and discharge measurements to compute
33
34 67 sediment fluxes in riverine and tidal environments (Suk et al., 1999, Ganju et al., 2005, Goni et
35
36 68 al., 2005, Ganju and Schoellhamer, 2006). For example, Ganju et al. (2005) used an acoustic
37
38 69 Doppler velocity meter (ADVM) to obtain water flux and, by using optical backscatter as a
39
40 70 proxy for suspended sediment concentration (SSC), estimated the suspended sediment flux over
41
42 71 spring-neap cycles from a tidal wetland in the Sacramento-San Joaquin River Delta. Boss and
43
44 72 Zaneveld (2003) coupled *in situ* measurements of velocity and colored dissolved organic matter
45
46 73 (CDOM) absorption to highlight the role of tides in fluxing CDOM away from the Bahamas
47
48 74 banks. Johnson et al. (2006) and Chapin et al. (2004) computed nitrate fluxes in a slough by
49
50 75 coupling a hydrological model with *in situ* measurements of nitrate estimated from absorption
51
52 76 measurements in the UV. The current study represents the first we are aware of that describes
53
54
55
56
57
58
59
60

1
2
3 77 use of combined optical and acoustic measurements to quantify fluxes of DOM as well as
4
5 78 document changes of DOM composition.
6
7

8 79 A major aim of the study was to develop a robust protocol for using optical and hydrologic
9
10 80 measurements to quantify concentrations and fluxes of dissolved organic carbon (DOC) in tidal
11
12 81 wetland systems. Determination of DOC flux in tidal environments is particularly difficult
13
14 82 because of the variability in concentration, owing to tidal, meteorological, and climatic forcing.
15
16 83 To assess the capabilities and limitations of the approach, we collected data during multi-week
17
18 84 deployments from a wetland channel adjacent to the San Francisco Estuary. Discrete samples
19
20 85 were collected systematically through the deployment for measurement of DOC and optical
21
22 86 parameters in the laboratory. The data was used to establish the relationships between measured
23
24 87 values of optical properties and DOC concentration. Comparison between in-situ and laboratory
25
26 88 optical properties validated that the in-situ optical measurements were not significantly affected
27
28 89 by biofouling.
29
30
31
32

33 34 90 ***Materials and procedures***

35 36 91 *Study location*

37
38 92 Browns Island is a natural tidal wetland in the San Francisco Bay estuary. The 2.8 km²
39
40 93 wetland is located near the confluence of the Sacramento River, San Joaquin River, and Suisun
41
42 94 Bay, approximately 77 km from the estuary mouth. Island vegetation is dominated by
43
44 95 tules/hardstem bulrushes (*Scirpus californicus* and *S. acutus*), cattails (*Typha angustifolia*),
45
46 96 saltgrass (*Distichlis spicata*) and other sedges growing on deep peat soils.
47
48
49

50 97 Browns Island contains a well-defined main channel with numerous side channels (Fig. 1).
51
52 98 Tides in this area are mixed semidiurnal, with a maximum spring tidal range of 1.8 m and a
53
54 99 minimum neap tide range of 0.20 m. At high water, the main channel is approximately 17 m
55
56
57
58
59
60

1
2
3 100 wide with a maximum depth of 4.5 m. This channel opens to the west, in the direction of tidal
4
5 101 inflow, and terminates at a lagoon in the eastern wetland interior. The main-channel sampling
6
7 102 site was upstream of major side channels approximately 300 m from the channel mouth (Fig.1).
8
9 103 Instrumentation was moored on the channel bottom at the center of the main drainage channel.
10
11

12 104 *Sampling procedure*

13
14
15 105 Acoustic and optical instrument packages were deployed in the Browns Island main channel
16
17 106 approximately 15 m apart for a four-week period in the winter, January-February 2006, and left
18
19 107 unattended except for weekly service visits to download data, clean optical sensors and replace
20
21 108 filter cartridges. Sampling periods were longer than two weeks in order to resolve the spring-
22
23 109 neap frequency of the tides.
24
25
26

27 110 During the sampling period, discrete samples were collected hourly for a 26 hour period
28
29 111 during the time of greatest tidal range to capture the maximum variability in DOC concentration
30
31 112 and character (Ganju et al., 2005). Laboratory measurements of light absorption and DOC were
32
33 113 then cross-calibrated with the accompanying *in situ* optical measurements.
34
35

36 114 *Moored optical system*

37
38
39 115 The optical instrument package consisted of a stainless steel cage containing submersible
40
41 116 sampling pumps, membrane filters, and optical and hydrographic sensors (Fig. 2).
42
43 117 Measurements were collected over multiple weeks at 30 min intervals by pumping water through
44
45 118 a 9 wavelength visible spectrophotometer (WET Labs ac-9 spectrophotometer; WET Labs,
46
47 119 Philomath, OR, USA), and a CDOM fluorometer (WET Labs WETStar, excitation wavelength
48
49 120 of 370 nm, emission wavelength nominal bandpass 460 nm). Water was pumped simultaneously
50
51 121 through a filtered flowpath for measurement of optical properties related to dissolved
52
53 122 constituents and an unfiltered flowpath for characterization of particulates. Conductivity,
54
55
56
57
58
59
60

1
2
3 123 salinity and pressure were measured with a Sea-Bird model SB37-SI CTD (Sea-Bird Electronics,
4
5 124 Bellevue, WA, USA). Pumps and instruments were controlled and most data logged using an *in*
6
7
8 125 *situ* data and power handler (DH-4, WET Labs). CTD data were collected using their onboard
9
10 126 dataloggers.

12 127 *Filtration and pumping system.*

15 128 For measurements of dissolved components, water was drawn through a pre-filter (Osmonics
16 129 model Memtrex, 25 cm length, 10 μm pore size; Osmonics, Osmonics, Inc., Minnetonka, MN,
17 130 USA) and then drawn through a finer filter (Osmonics model Memtrex, 25 cm length, 0.2 μm
18 131 pore size; Osmonics, Inc., Minnetonka, MN, USA) using a SHURflo model 1100 pump
19 132 (SHURflo, Cypress, CA, USA) modified by the addition of a submersible power relay. These
20 133 waters were then drawn through the absorption (*a*) flow cell of the ac-9 and the WETStar
21 134 fluorometer. In the non-filtered flowpath, a single Sea-Bird 5T pump (Sea-Bird Electronics,
22 135 Bellevue, WA, USA) with a Teflon screen (1 mm mesh size, to exclude very large detritus) was
23 136 used to draw samples through the Sea-Bird SB37-SI CTD and the attenuation (*c*) flow cell of the
24 137 ac-9.

27 138 The flow-through instruments were connected using Tygon plasticizer-free tubing (Saint-
28 139 Gobain Performance Plastics, www.tygon.com) pre-rinsed with dilute HCl and organic-free
29 140 water. The clear tubing was wrapped with black electrical tape to minimize the effects of
30 141 external light biasing the sensitive ac-9 photometer. The tape-wrapped tubing was also soaked
31 142 overnight in organic-free water to leach possible contaminants from the tape.

32 143 In the field, tubing and filters were replaced every week, following the data download and
33 144 instrumentation servicing/cleaning to minimize the effects of biological fouling.

34 145 *CDOM absorption.*

1
2
3 146 Absorption by chromophoric dissolved material (CDOM) was measured at nine visible
4
5 147 wavelengths by the WET Labs ac-9 spectrophotometer: 412, 440, 488, 510, 532, 555, 650, 676,
6
7
8 148 and 715 nm. The protocol for ac-9 data collection and processing of Twardowski et al. 1999 was
9
10 149 modified to accommodate the relatively high DOC and particulate loads of the Browns Island
11
12 150 waters. A larger (5 m²) 0.2 µm membrane filter and a 10 µm pre-filter was used as well as 10 cm
13
14 151 pathlength ac-9. The large filtration cartridge permitted longer deployments than would have
15
16 152 been possible with smaller filters. The shorter flow cell was needed because of the high DOC
17
18 153 concentration. The ac-9 flow cells and detectors (absorption flow cell and attenuation flow cell)
19
20 154 were cleaned using a combination of lens papers, 0.5% solution of Liquinox[®], and organic-free
21
22 155 water, plus a final rinse of organic-free water. Pure water offsets were checked in the lab before
23
24 156 and after each field deployment, and monitored in the field by logging air reading before and
25
26 157 after weekly service.

27
28
29
30
31 158 *CDOM fluorescence (FDOM).*

32
33
34 159 The fluorescent fraction of the DOM pool (FDOM) was measured *in situ* using a WET Labs
35
36 160 WETStar single-band excitation-emission *in situ* fluorometer (370 nm excitation, 10 nm full
37
38 161 width half max, FWHM; 460 nm emission, 120 nm FWHM). The fluorometer was installed in
39
40 162 the filtered path after the ac-9. The fluorometer flowpath was cleaned using lens papers, 0.5%
41
42 163 solution of Liquinox[®], and organic-free water, plus a final rinse of organic-free water as
43
44 164 described in the users' guide provided by WET Labs. Blank water offsets were collected before
45
46 165 every field deployment and subtracted from the field measurements. Raw data collected from
47
48 166 the WETStar fluorometer were converted from volts DC (VDC) to quinine sulfate units (QSU)
49
50 167 using the factory-supplied QSU scale factor (units of µg L⁻¹).

51
52
53 168 *CDOM composition.*
54
55
56
57
58
59
60

1
2
3 169 Two optical parameters associated with DOM composition, spectral slope (S) and relative
4
5
6 170 fluorescence efficiency (RFE, Blough and Green 1995, Klinkhammer et al. 2000, Blough and
7
8 171 Del Vecchio 2002;) were calculated. S has been shown to increase with decreasing bulk
9
10
11 172 molecular weight (Carder et al. 1989; Yacobi et al. 2003) or with decreasing aromatic content.
12
13 173 These two parameters have also been used to identify DOC originating from different sources
14
15 174 (terrestrial versus marine) and to characterize processes affecting the DOC pool (e.g. photo-
16
17 175 oxidation, primary production; Vodacek and Blough, 1997, Twardowski and Donaghay 2001).

18
19
20 176 S was calculated using a non-linear spectral fit of an exponential function with a baseline
21
22 177 offset correction (Chen, et al., 2007) to the absorption spectrum in the range of 440-676 nm
23
24 178 using the *fminsearch* function in MATLAB:

25

$$26 \quad 27 \quad 28 \quad 29 \quad 30 \quad 31 \quad 32 \quad 33 \quad 34 \quad 35 \quad 36 \quad 37 \quad 38 \quad 39 \quad 40 \quad 41 \quad 42 \quad 43 \quad 44 \quad 45 \quad 46 \quad 47 \quad 48 \quad 49 \quad 50 \quad 51 \quad 52 \quad 53 \quad 54 \quad 55 \quad 56 \quad 57 \quad 58 \quad 59 \quad 60$$
$$180 \quad a_g(\lambda) = a_g(\lambda_{ref}) \exp[-S(\lambda - \lambda_{ref})] + K \quad (1)$$

181
182 where $a_g(\lambda)$ is the absorption coefficient of CDOM at a specified wavelength, λ_{ref} is a reference
183 wavelength, S is the slope fitting parameter and K is the offset correction, also calculated by
184 *fminsearch* in MATLAB. We opted to fit the absorption spectra using the exponential fit (e.g.
185 Blough and Del Vecchio 2002; Babin et al., 2003, Twardowski et al. 2004) and a spectrally fitted
186 offset, K , as an alternative to offset correction methods (e.g. Bricaud et al, 1981), using
187 subtraction of absorption in the red (see discussion section below).

188 Relative fluorescence efficiency (RFE) ($\mu\text{g L}^{-1}$ quinine sulfate m^{-1}) was calculated as the ratio
189 of the CDOM fluorescence (excited at 370 nm) to the CDOM absorption at 370 nm (a_{g370} ; m^{-1})
190 extrapolated from the ac9 spectra via the spectral slope.

191 *Attenuation of visible light.*

1
2
3 192 The unfiltered attenuation flow cell of the ac-9 provided measurements of total attenuation,
4
5
6 193 that is the sum of absorption and scattering by both dissolved and particulate material.

7
8 194 *Power, control and data logging.*

9
10 195 Most *in situ* optical instrumentation and data were controlled, logged, and time-stamped
11
12 196 using a WET Labs model DH-4 data handler. The DH-4 was programmed to take field
13
14
15 197 measurements every 30 minutes, with each data-collection interval consisting of a one-minute
16
17 198 pumping pre-flush and instrument-warming period followed by a one-minute sampling period.
18
19
20 199 The DH-4 is designed to provide power to pumps and sensors with a 1.25 Amp maximum
21
22 200 output. The SHURflo model pump in the filtered flowpath draws approximately 4.0 Amps at 12
23
24 201 Vdc and required an external solid-state relay device to power the pump without damaging the
25
26
27 202 DH-4. Power (12 Vdc) was supplied using a land-moored battery package. Total equipment
28
29 203 power consumption was 6.5 amperes, resulting in 10.4 amp-hours needed each day and thus
30
31 204 required 2–100 amp-hour batteries in parallel to operate continuously over a seven-day period.
32
33
34 205 To ensure reliable power supply over a one-week service interval, we used four 100 amp-hour
35
36 206 batteries instrumented in parallel.

37
38
39 207 *Hydrological measurements*

40
41 208 The CTD measuring temperature salinity and pressure was deployed on the channel bottom as
42
43 209 previously described by Ganju et al. (2005). Water velocity measurements were made using a
44
45
46 210 Sontek Argonaut XR upward-looking acoustic Doppler velocity meter (ADV) (Sontek/YSI,
47
48 211 San Diego, CA, USA) deployed on the main channel bed. The ADV was programmed to
49
50 212 collect the depth-averaged velocity and water depth above the unit for 6 min during the
51
52
53 213 beginning of every 15 min period as well as the water depth. Surveys using a downward-looking
54
55 214 acoustic Doppler profiler provided the cross-sectional width ($W(z,t)$) of the channel as a function
56
57
58
59
60

1
2
3 215 of depth (z , at each tidal phase) as well as the along channel velocity and were used to compute
4
5
6 216 the along channel averaged velocity $u(t)$.

7
8 217 *Discrete Water Sampling*

9
10 218 Discrete water samples were taken hourly over a 24 hour period, over a maximum tidal range
11
12 219 to provide data for the *in situ* optical measurements as well as biogeochemical analysis. The
13
14
15 220 intent was to collect data on concentration and composition over the dynamic range encountered
16
17 221 *in situ* during an entire tidal cycle. Discrete samples were also collected during a shorter period
18
19
20 222 two weeks earlier to assess possible changes in the biogeochemistry/optics relationships over two
21
22 223 weeks.

23
24 224 Since concentrations and velocities may vary across and with depth in the tidal channel,
25
26 225 water samples were collected using an isokinetic D-77 bottle sampler with a ¼-inch nozzle
27
28 226 (Edwards and Glysson 1999). Equal discharge increment (EDI) sampling based on five equally
29
30 227 spaced centroids was used to represent the average conditions in the main channel. The sampler
31
32
33 228 was lowered to just above the sediment–water interface and then raised to the surface at a rate
34
35
36 229 such that an equal volume of water was collected at each centroid location, providing a vertically
37
38 230 integrated sample at five points across the channel. All samples were gravity-filtered in the field
39
40
41 231 as quickly as practical through precombusted 47 mm diameter, 0.3 μm pore-size glass fiber
42
43 232 filters (GFF) (Advantec MFS model GF-7547mm; Advantec MFS, Dublin, CA, USA) into
44
45 233 carbon-free, precombusted glass vials and immediately packed on ice. The resulting
46
47
48 234 concentration theoretically equals the cross sectionally (horizontally and vertically) averaged
49
50
51 235 velocity-weighted concentration ($C(t)$).

52
53 236 *Laboratory measurements*

54
55 237 *DOC*

1
2
3 238 DOM measurements are expressed here as dissolved organic carbon (DOC) concentration,
4
5
6 239 measured on filtered samples using a Shimadzu TOC-5000A total organic carbon analyzer
7
8 240 (Shimadzu, Columbia, MD, USA) according to the method of Bird et al. (2003). Each DOC
9
10 241 analysis represents the mean of three or more injections. The instrument gave consistent blank
11
12 242 values of $< 0.05 \text{ mg L}^{-1}$ carbon. Uncertainty in our laboratory DOC measurement is estimated to
13
14
15 243 be 3% of the measured value for samples with concentrations $> 1 \text{ mg L}^{-1}$ (Bird et al, 2003), based
16
17 244 on the precision of the analytical technique and the uncertainty in the blank and replicate
18
19
20 245 measurements.

21 22 246 *Data Processing and Calculations*

23
24
25 247 Raw data from all *in situ* sensors were merged together to the common time of the CTD,
26
27 248 which had the lowest sampling frequency (1.16 Hz). Data were then binned by averaging the
28
29 249 final twenty seconds of each one minute sampling interval. The forty seconds of data at the
30
31
32 250 outset of each sampling interval were used as a quality control measure to ensure *in situ* pumping
33
34 251 rates were sufficient to clear the flowpath during the instrument warm up period.

35
36 252 Following data merging and binning, standard temperature corrections were applied to the ac-9
37
38 253 data (Pegau et al. 1997). Deionized, organic-free water blanks (Hydro Picosystem Plus; Hydro,
39
40 254 Durham, NC, USA) were measured by both lab and field instruments and were subtracted from
41
42
43 255 the respective fluorometer and spectrophotometer values. Weekly service gaps in the *in situ* data
44
45
46 256 record (typically about two hours in duration, due to the weekly data downloads and servicing)
47
48 257 were interpolated using linear interpolation in MATLAB.

49 50 258 *Flux calculations*

51
52
53 259 The water flux through the channel was taken to be the integral of the velocity, $u(t)$, in the
54
55 260 cross section:

$$261 \quad Q(t) = \int u \, dA \quad (2)$$

262 Where u is the along-channel averaged velocity and A the cross sectional area. The EDI
 263 sampling procedure described above provided the cross-sectionally averaged concentration:

$$264 \quad C(t) = \frac{\int uc \, dA}{\int u \, dA} \quad (3)$$

265 in which c is the concentration of a constituent (here DOC). The numerator of equation 3 is the
 266 constituent flux (DOC flux) through the cross-section with units of mass per unit time. The
 267 denominator of equation 3 is the water discharge $Q(t)$ (equation 2). Thus, flux was given by the
 268 product of $C(t)$ and $Q(t)$. $C(t)$ was calculated from the optical surrogate time series calibrated to
 269 the EDI samples, and $Q(t)$ was available from the calibrated ADVm time series.

270 **Assessment**

271 *Discrete Measurements: Variation in DOC Concentration*

272 DOC concentrations in the tidal channel varied tidally. For example, 25 discrete samples
 273 collected during the winter deployment ranged from 2.5 to 3.9 mg L⁻¹ (Fig.3). The higher DOC
 274 concentrations were observed during the low flows of ebb tide while lower concentrations (2.5
 275 mg L⁻¹) occurred during higher flows of flood tides.

276 *Optical properties*

277 Optical properties varied tidally with FDOM ranging from 65 QSU ppb during flood to 110
 278 QSU ppb during ebb (Fig. 3). Absorption coefficients measured at 440 nm (a_{g440}) exhibited
 279 similar periodicity and the variability was coherent with that of FDOM (Fig.3). Intercalibration
 280 of in-situ CDOM absorption and laboratory absorption ranged from $R^2 = 0.97 - 0.99$.

281 *Relation between DOC and field optical measurements*

1
2
3 282 Several of the optical measurements were strongly related to the DOC concentration for the
4
5
6 283 deployment period. While deviations between each measurement were observed, the general
7
8 284 agreement between the field optical measurements and lab measured DOC concentration is
9
10 285 highly significant (Fig. 4).

11 12 286 *Multivariate correlation and DOC prediction*

13
14
15 287 The generally good relationship between DOC concentration and optical proxies, FDOM, a_g440 ,
16
17 288 and a_g650 , (Fig. 4) shows the utility of even single optical measurements as predictors of DOC.
18
19
20 289 However, using multiple optical property values to predict DOC concentrations resulted in a
21
22 290 significantly better correlated predictive tool.

23
24
25 291 We used a partial least squares regression (PLS1; The Unscrambler 9.2; Camo Technologies,
26
27 292 Woodbridge, NJ, USA) to relate values of 17 optical properties to measured DOC concentrations
28
29 293 (Fig. 5). We obtained the best results using measured values for CDOM fluorescence (ex370nm
30
31 294 / em 460 nm); CDOM absorption from the ac-9 at 8 wavelengths ($a_g412 - a_g656$ nm); and total
32
33 295 attenuation from the ac-9 at 8 wavelengths ($c412 - c656$ nm). The model was fully cross-
34
35
36 296 validated and no pretreatments to the variables such as weighting or normalization were used.
37
38
39 297 Model predictions were within +/- 0.2 mg L⁻¹ of the measured value for three discrete DOC
40
41 298 measurements obtained on January 19, 2006 and not part of the model calibration set.

42 43 44 299 *DOC time series*

45
46 300 The PLS regression model was used to convert high-frequency time series of optical data to
47
48 301 modeled *in situ* DOC concentrations (Fig. 6A). The time series of DOC concentration is very
49
50 302 non-symmetric with respect to the tide. DOC values were highest at the lowest water depths and
51
52 303 decreased with increasing depth (Fig. 6A). This pattern suggests that DOC concentration and
53
54
55 304 source are dominated by wetland sediment porewater rather than circulating water forced by tide.
56
57
58
59
60

1
2
3 305 In other words, as water depth in the channel decreases, sediment porewater drains into the
4
5 306 channel, elevating DOC values. DOC concentrations are therefore maximal when water levels
6
7
8 307 are lowest.
9

10 308 *Discharge*

11
12 309 The water discharge time series shows flood and ebb tides somewhat symmetrical, dominated
13
14
15 310 by flood tide discharge by approximately 3.5 percent by volume. In contrast, the peak
16
17 311 instantaneous ebb flows were 20 percent greater than flood flows (Fig. 6B). Spring tides occur
18
19 312 on 1/15/06 and 1/31/06 while the neap tide occurs on 1/23/06. The full spring-neap range and
20
21 313 the accompanying complete matching DOC concentration time series are needed to calculate the
22
23 314 DOC flux over this period.
24
25

26 315 *DOC flux*

27
28 316 Instantaneous DOC flux is dominated by the tidal discharge which is, in general, more
29
30 317 semidiurnally dominated and symmetrical than the DOC concentration (Fig. 6C). The 14.7 day
31
32 318 (spring-neap) integrated flux varied over time, in response to physical forcings (Fig. 6D).
33
34 319 Although there was a net off-island transport of DOC over this time period, the flux varied both
35
36 320 in sign and in magnitude, depending on the specific period of integration in the time series. This
37
38 321 demonstrates that discrete sampling over one or a few tidal cycles cannot capture the true
39
40 322 variability in flux. Net DOC flux must be calculated at least over a full spring–neap period (14.7
41
42 323 days) and even then the choice of start time matters. It is important to select starting and ending
43
44 324 times with similar water depths since this minimizes biases.
45
46
47
48
49

50 325 *Uncertainties in DOC flux*

51
52 326 The uncertainty in DOC flux was calculated analogously to that presented in Ganju et al. for
53
54 327 sediment flux (2005), and was found to be less than 25% (based on a 3% uncertainty in modeled
55
56
57
58
59
60

1
2
3 328 DOC values) and assuming the uncertainties in water velocity and modeled DOC to be
4
5 329 uncorrelated. This is compared to a calculated uncertainty in the sediment flux of sediments of
6
7
8 330 27%, as presented previously (Ganju et al., 2005).
9

10 331 *Effect of sampling interval*

11
12 332 To evaluate the extent to which the choice of beginning and end time made for calculating net
13
14 333 DOC flux, we recalculated the flux for all the full spring–neap periods ($\Delta t \sim 14.7$ day) within a
15
16 334 representative time series (~ 21 day; 22 cycles total). We found the calculated net DOC flux off
17
18 335 the wetland over the 22 ‘optimal’ cycles to vary from 0.9×10^6 g C to 2.9×10^6 g C, with a mean
19
20 336 of 1.8×10^6 g C, indicating that the specific time period chosen affected the calculated flux, and
21
22 337 that the value of flux provided above could be biased by as much as a factor of three if we were
23
24 338 to measure the spring–neap flux over a single 14.7 day interval. Time series greater than the
25
26 339 spring–neap interval are thus recommended.
27
28
29
30
31

32
33 340 To assess the effect of sampling interval on DOC flux, we subsampled the modeled DOC time
34
35 341 series at successively larger intervals, and then interpolated back the data to the 15 min water
36
37 342 flux data (to avoid confounding physical sampling with the optics). We found a cubic-spline
38
39 343 interpolation (as implemented in MatLab) to consistently outperform linear interpolation, and we
40
41 344 show only results using that interpolation method. Averaged over the 22 possible spring–neap
42
43 345 cycles, we found no significant deterioration in the flux estimate for sampling intervals of 90 min
44
45 346 or less (Fig. 7). For sampling intervals of three hours or more biases larger than 20% were
46
47 347 common.
48
49
50

51 52 348 *Dynamics of DOM optical character*

53
54
55 349 DOM quality parameters also varied over tidal and spring–neap time scales. Time series of
56
57 350 the spectral slope, S , exhibited lower values during ebb tides (commonly associated with high
58
59
60

1
2
3 351 molecular weight DOM) and higher values during flood tides. This is consistent with changes in
4
5 352 DOM composition (associated with lower molecular weight DOM, e.g. Carder et al. 1989,
6
7
8 353 Yacobi et al. 2003) associated with tidal forcing and sources—riverine inputs via the Sacramento
9
10 354 and San Joaquin Rivers during flood tides and mixtures of wetland and riverine waters during
11
12 355 ebb tides (Fig. 8). Lower S values are associated with higher DOC concentrations measured
13
14
15 356 during ebb tides and higher S with lower DOC concentrations over flood tides.

17 357 *Relative fluorescence efficiency*

18
19
20 358 The time series of RFE (Fig.8), like that of the CDOM spectral slope, shows evidence of
21
22 359 tidally forced changes in DOM composition and are consistent with the observed S time series
23
24 360 (Fig 8). Linear regression of FDOM (370nm) with absorption (a_g370) were well correlated ($R^2 =$
25
26 361 0.98) with a regression slope of 16, similar to reported values for RFE of CDOM in estuaries
27
28 362 (Klinkhammer et al., 2000 and Chen et al., 2007). The time series of RFE (Fig.8) displays lower
29
30 363 RFE values consistent with wetland porewater entering the channel during ebb tides.

33 364 *Discussion*

34
35
36 365 An optical instrumentation package was designed and deployed to obtain continuous, high-
37
38 366 quality DOM estimates over time scales ranging from minutes to weeks. In a shallow, sediment-
39
40 367 loaded slough, the package performed remarkably well and provided high-quality measurements
41
42 368 of dissolved optical properties. Several of the optical measurements were found to provide an
43
44 369 excellent proxy for DOC, which improved with the use of a multivariate predictive model.
45
46 370 Concurrent discharge measurements allowed us to calculate quantitative estimates of DOC flux.
47
48 371 In-situ multi-spectral measurements of filtered absorption and fluorescence allowed us to
49
50 372 examine the time-dependent compositional evolution in DOM as source contributions varied
51
52 373 (e.g., wetland porewaters versus riverine sources).

1
2
3 374 We used a spectral model (Eq. 1) to obtain the spectral slope and baseline offsets. We
4
5 375 compared this method with another method of correcting absorption offsets and effects on
6
7
8 376 spectral slope (S)—subtracting absorption in the red (e.g. a_{715}) from the a_{412} – a_{715} nm (e.g.
9
10 377 Babin et al., 2003); Although both techniques yielded similar, though not identical, results in
11
12 378 both the offset value (essentially a_{715}), and S , we preferred Eq. 1 as it does not assume
13
14
15 379 $a_g(715)=0$ for these high CDOM laden waters. Further work needs to be completed to
16
17 380 substantiate that this correction is superior. However, for the purpose of obtaining DOC
18
19 381 concentration using the PLS analysis, both methods as well as no baseline correction provided
20
21 382 similar quality fits (most likely due to the inclusion of the attenuation data in the PLS analysis
22
23 383 that substantially increased the quality of the fit).

24
25
26
27 384 Assessment of the method indicates that DOM can be reliably measured *in situ* by optical
28
29 385 means over timescales ranging from minutes to months. Measurements at these timescales allow
30
31 386 investigation of many biogeochemical processes, including those related to carbon and nitrogen
32
33 387 cycling (e.g., primary production, biodegradation and photodegradation, and interaction with
34
35 388 trace metals and pesticides)—processes that are important to aquatic and marine food webs and
36
37 389 to drinking water quality.

38
39
40
41 390 Methods utilizing high-frequency sampling can also capture the occurrence and consequences
42
43 391 of episodic but important events that might be missed with less frequent discrete sampling. For
44
45 392 example, even weekly field sampling may miss brief forcing events such as precipitation, or
46
47 393 changes in prevailing winds that may result in significant resuspension of sediments containing
48
49 394 DOM.

50
51
52
53 395 The method presented here was designed to provide a high-frequency view of not only DOC
54
55 396 concentrations, but also optical surrogates for DOM character. The *in situ* optical measurements
56
57
58
59
60

1
2
3 397 enabled differentiation of incoming and outgoing DOC and thus contributed to an improved
4
5 398 understanding of the underlying processes regulating DOC concentration and character.
6
7
8 399 This study demonstrated that redundancy is an important element in designing optical-
9
10 400 hydrologic packages to characterize biogeochemical quantities, character, and fluxes (for
11
12 401 example, CDOM fluorescence and CDOM absorption). It is important to include in the package
13
14 402 design a number of measurements looking at the same parameter from different "points of view".
15
16
17 403 Selecting an appropriate sampling interval—appropriate to the targeted biogeochemical
18
19 404 processes and to the environment of deployment—is another important element. By sampling at
20
21 405 high frequency (every 30 min in this case) and then sub sampling the resulting high-frequency
22
23 406 time-series at a range of intervals, we determined that we could have—in the case of the Browns
24
25 407 Island channel—sampled every ninety minutes and achieved similar results (Fig. 7). Sampling at
26
27 408 intervals > 90 min would have resulted in a significant degradation of results.
28
29
30

31 409 One challenge for the future will be extending deployment duration. The use of multiple filters
32
33 410 that can automatically be changed as filtration capabilities degrade is a possible solution.
34
35 411 Automated cleaning and field calibration (e.g., periodic automatic injection of cleaning fluid and
36
37 412 then deionized water) would also extend deployment capabilities. Lengthier deployments will
38
39 413 likely require collection of additional calibration and validation samples to insure that the link
40
41 414 between optics and biochemistry is robust.
42
43
44

45 415 *Comments and recommendations*

46
47 416 The sampling method described here is intended to supplement discrete sampling analysis, and
48
49 417 thus great care should be taken to adapt the instrument package to the environment, and to
50
51 418 establish the relationships between the measured optical properties (proxies) and DOC or any
52
53 419 other biogeochemical parameters of interest. We found that multiple overlapping measurements
54
55
56
57
58
59
60

1
2
3 420 were useful for establishing robust models useful for extrapolation and interpolation of time
4
5
6 421 series data.
7

8 422 *Filtration system design*—Since several of the core optical parameters are related to dissolved
9
10 423 constituents (e.g., CDOM spectral slope, FDOM), particular care must be devoted to finding a
11
12 424 filtration system appropriate to the deployment environment. In the case of the Browns Island
13
14 425 channel—a tidal channel with elevated particulate concentrations—we achieved long
15
16 426 deployment periods only through addition of large surface area filters and weekly service
17
18 427 intervals. This would be impractical for many studies.
19
20

21
22 428 *Sampling interval*—At Browns Island, we found that the sampling interval of the optical
23
24 429 properties could be as great as 90 minutes without significant loss of DOC flux data quality
25
26 430 (compared to 30 min. intervals). This threshold, however, would be expected to vary by
27
28 431 environment and probably seasonally as well. Any new deployment should therefore initially
29
30 432 include high-frequency sampling, plus calculations (Fig. 7) to determine whether less frequent
31
32 433 sampling could be conducted without significant degradation of data quality. Less frequent
33
34 434 sampling can extend battery and filter life and can therefore facilitate less frequent service visits
35
36 435 and perhaps longer deployments if biofouling is not observed. The interval at which field
37
38 436 samples must be collected for model calibration will also be a function of environment and
39
40 437 season.
41
42
43
44
45
46
47
48
49
50
51
52
53
54
55
56
57
58
59
60

438 *Acknowledgements*

439 This work was funded as part of the CALFED Science Strategy Plan for the Bay-Delta
440 Ecosystem. This study would not have been possible without the assistance of key personnel of
441 the USGS CA Water Science Center. Special thanks go out to Gail Wheeler, Kathryn Crepeau,
442 Susan Bird, Will Kerlin, Miranda Fram for laboratory and field assistance and Donna Knifong
443 for illustration assistance. We also thank Tonya Clayton, Tamara Kraus, Brian Pellerin, and
444 Robert Spencer for their insightful reviews of earlier versions of the manuscript, and many others
445 for their helpful discussions. Finally, we would like to thank the ONR for funding the
446 instrumentation used in this study. The use of brand or firm names in this paper are for
447 identification purposes only and do not constitute endorsement by the U.S. Geological Survey.

448 **References**

- 449 Aiken, G. R., D. M. McKnight, R. L. Wershaw, and P. MacCarthy. 1985. Humic substances in
450 soil, sediment and water. John Wiley and Sons.
- 451 Bird, S. M., M. S. Fram, and K. L. Crepeau. 2003. Method of analysis by the U.S. Geological
452 Survey California District Sacramento Laboratory—determination of dissolved organic
453 carbon in water by high temperature catalytic oxidation, method validation, and quality-
454 control practices. U.S. Geological Survey Open-file report 03-366. U.S. Geological
455 Survey.
- 456 Babin, M.D., Stramski, G.M., Ferrari, H. Claustre, A. Bricaud, G. Oblesky and N. Hoepffner.
457 2003. Variations in the light absorption coefficients of phytoplankton, non-algal particles,
458 and dissolved organic matter in coastal waters around Europe. *J. Geophys. Res.*,
459 108(C7), 3211.
- 460 Blough, N.V., and S. A. Green. 1995. Spectroscopic characterization and remote sensing of
461 NLOM, p. 23-45. *In* R. G. Zepp and C. Sonntag [eds.], *The role of non-living organic*
462 *matter in the earth's carbon cycle*. John Wiley and Sons.
- 463 Blough, N. V., and R. Del Vecchio. 2002. Distribution and dynamics of chromophoric dissolved
464 organic matter (CDOM) in the coastal environment, p. 509-546. *In* D. A. Hansell, and C.
465 A. Carlson [eds.], *Biogeochemistry of marine dissolved organic matter*. Academic Press.
- 466 Boss E. and J. R. V. Zaneveld. 2003. The effect of bottom substrate on inherent optical
467 properties: evidence of biogeochemical processes. *Limnol. Oceanogr.* 48(1): 346-354.
- 468 Boss, E., R. Collier, G. Larson, K. Fennel, and W.S. Pegau. 2007. Measurements of spectral
469 optical properties and their relation to biogeochemical variables and processes in Crater
470 Lake National Park, OR. *Hydrobiologia* (2007), 574:149-159.

- 1
2
3 471 Bricaud, A., A. Morel, and L. Prieur. 1981. Absorption by dissolved organic matter of the sea
4
5 472 (yellow substance) in the UV and visible domains. *Limnol. Oceanogr.* 26 (1): 43–53.
6
7
8 473 Carder, K. L., R. G. Steward, G. R. Harvey, and P. B. Ortner. 1989. Marine humic and fulvic
9
10 474 acids: their effects on remote sensing of ocean chlorophyll. *Limnol. Oceanogr.* 34:68-81.
11
12 475 Chapin, T. P., J. M. Caffrey, H. W. Jannasch, L. J. Coletti, J. C. Haskins, and K. S. Johnson,
13
14 476 2004. Nitrate sources and sinks in Elkhorn Slough, California: results from long-term
15
16 477 continuous in situ nitrate analyzers. *Estuaries* 27(5):882–894.
17
18
19 478 Chen, Z., Hu, C., R.N. Conmy, F. Muller-Karger, and P. Swarzenzki. 2007. Colored dissolved
20
21 479 organic matter in Tampa Bay, Florida. *Marine Chemistry* 104, 98-109.
22
23
24 480 Claustre, H., A. Sciandra, and D.Vaulot. 2008. Introduction to the special section bio-optical and
25
26 481 biogeochemical conditions in the South East Pacific in late 2004: the BIOSOPE program,
27
28 482 *Biogeosciences*, 5, 679-691.
29
30
31 483 Dickey, T. 2001. New technologies and their roles in advancing recent biogeochemical studies,
32
33 484 *Oceanogr.* 14(4):108-120.
34
35
36 485 Edwards, T. K. and G. D. Glysson. 1999. Field methods for measurement of fluvial sediment, p.
37
38 486 1–89. In *Techniques of Water-Resources Investigations*, Book 3. U.S. Geological Survey,
39
40 487 Reston, Virginia.
41
42
43 488 Ganju, N. K., D. H. Schoellhamer, and B. A. Bergamaschi. 2005. Suspended sediment fluxes in a
44
45 489 tidal wetland: measurement, controlling factors and error analysis. *Estuaries* 28(6):812-
46
47 490 822.
48
49
50 491 Ganju, N.K., and D.H. Schoellhamer. 2006. Annual sediment flux estimates in a tidal strait using
51
52 492 surrogate measurements: *Estuarine, Coastal and Shelf Science*, v. 69, p. 165-178.
53
54
55
56
57
58
59
60

- 1
2
3 493 Goni, M.A., M.W. Cathey, Y.H. Kim and G. Voulgaris. 2005. Fluxes and sources of suspended
4
5
6 494 organic matter in an estuarine turbidity maximum region during low discharge
7
8 495 conditions. Estuarine, Coastal and Shelf Science 63: 683-700.
9
10 496 Johnson, K. S., L. J. Coletti, and F. P. Chavez. 2006. Diel nitrate cycles observed with in situ
11
12 497 sensors predict monthly and annual new production. Deep-Sea Res. Pt. I 53:561-573.
13
14
15 498 Klinkhammer, G.P., J. McManus, D. Colbert, and M.D. Rudnick. 2000. Behavior of terrestrial
16
17 499 dissolved organic matter at the continent-ocean boundary from high-resolution
18
19
20 500 distributions. Geochimica et Cosmochimica Acta, Vol 64, No 16, 2765-2774
21
22 501 Mantoura, R.F.C., A. Dickson and J.P. Riley. 1978. The complexation of metals with humic
23
24 502 materials in natural waters. Estuarine Coastal Shelf Sci. 6:387-408.
25
26
27 503 Pegau, W. S., D Gray, and J. R. V. Zaneveld. 1997. Absorption and attenuation of visible and
28
29 504 near-infrared light in water: dependence on temperature and salinity. Appl. Opt. **36**,
30
31 505 6035-6046.
32
33
34 506 Suk, N.S., Guo, Q., and N.P. Psuty. 1999. Suspended solids flux between salt marsh and adjacent
35
36 507 bay: A long-term continuous measurement. Estuarine, Coastal and Shelf Science. 49,61-
37
38 508 81.
39
40
41 509 Twardowski, M. S., J. M. Sullivan, P. L. Donaghay, and J. R. V. Zaneveld. 1999. Microscale
42
43 510 quantification of the absorption by dissolved and particulate material in coastal waters
44
45 511 with an ac-9. J. Atmos. Ocean. Technol. 16(12):691-707.
46
47
48 512 Twardowski, M. S. and P. L. Donaghay. 2001. Separating in situ and terrigenous sources of
49
50 513 absorption by dissolved materials in coastal waters. Jour.Geophys.Res. 106, C2:2545-
51
52 514 2560.
53
54
55
56
57
58
59
60

- 1
2
3 515 Twardowski, M. S., E. Boss, J. M. Sullivan, and P. L. Donaghay. 2004. Modeling the spectral
4
5
6 516 shape of absorption by chromophoric dissolved organic matter. *Mar. Chem.* 89:69-88.
7
8 517 Vodacek, A., and N. V. Blough. 1997. Seasonal variation of CDOM and DOC in the Middle
9
10 518 Atlantic Bight: terrestrial inputs and photooxidation. *Limnol. Oceanogr.* 42(4):674-686.
11
12 519 Yacobi, Y. Z., J. J. Alberts, M. Takács, and M. McElvaine. 2003. Absorption spectroscopy of
13
14
15 520 colored dissolved organic carbon in Georgia (USA) rivers: the impact of molecular size
16
17 521 distribution. *J. Limnol.* 62(1):41-46.
18
19
20
21
22
23
24
25
26
27
28
29
30
31
32
33
34
35
36
37
38
39
40
41
42
43
44
45
46
47
48
49
50
51
52
53
54
55
56
57
58
59
60

Fig. 1.

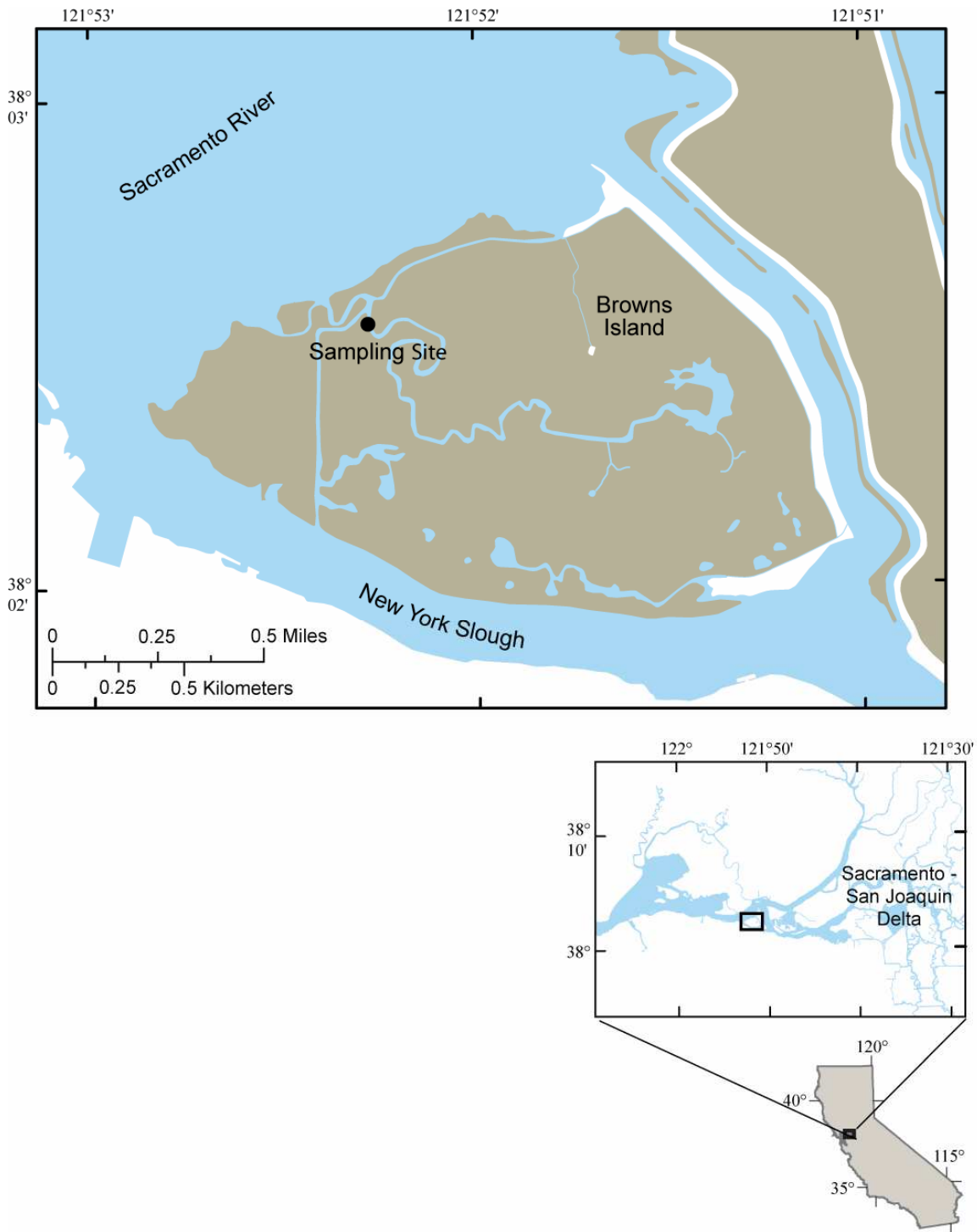


Figure 1: Browns Island study area, Sacramento – San Joaquin River Delta, California, USA.

1
2
3
4
5
6
7
8
9
10
11
12
13
14
15
16
17
18
19
20
21
22
23
24
25
26
27
28
29
30
31
32
33
34
35
36
37
38
39
40
41
42
43
44
45
46
47
48
49
50
51
52
53
54
55
56
57
58
59
60

Fig. 2.

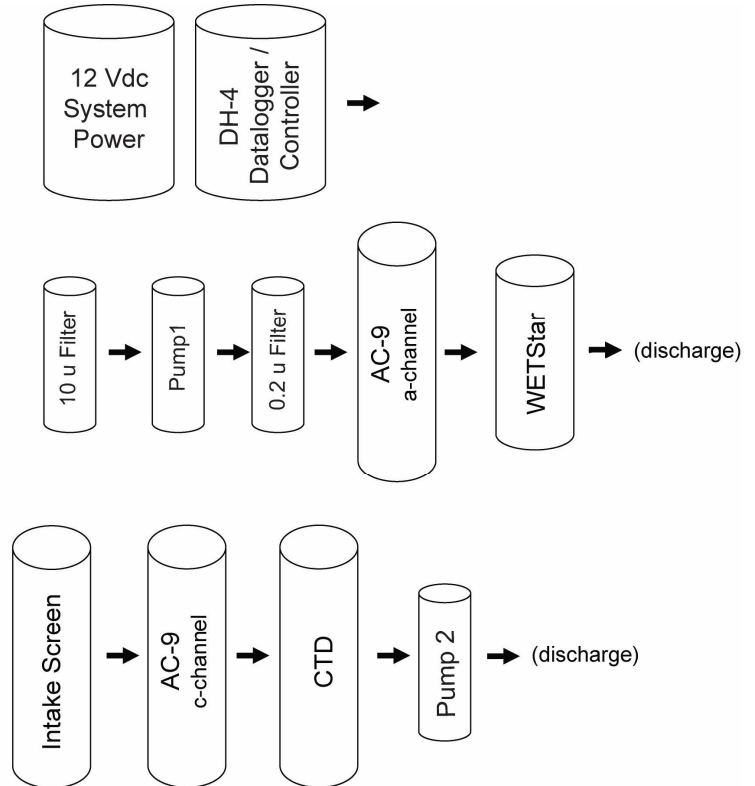


Figure 2: The optical instrument package is a parallel flow-through system with one filtered and one unfiltered channel, allowing simultaneous characterization of dissolved and particulate fractions within the water column. The system, which is capable of week-long deployments, autonomously measures absorption in the ultraviolet and visible spectra; absorption, backscatter, and attenuation in the visible spectrum; and CDOM, temperature, and water depth.

Fig. 3

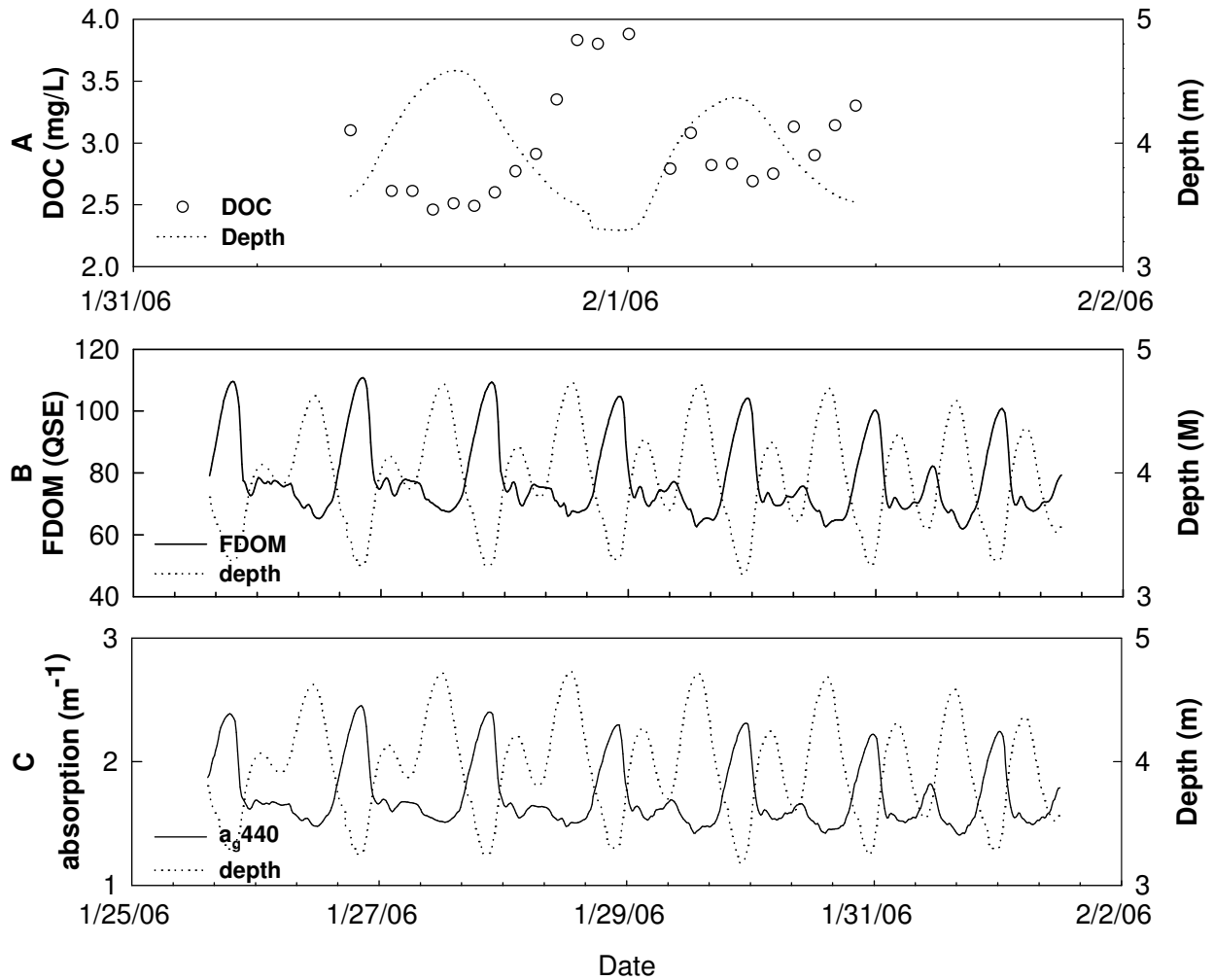


Figure 3: Fig 3A —Water depth and DOC (mg L⁻¹) concentrations measured over the 24 hour period of discrete sampling. DOC concentrations (open circles) were higher during ebb tide and lower during flood tide. Fig 3B and 3C —Continuous measurements display tidal variation in CDOM properties of FDOM (WETStar) and a_{440} (ac-9) from one week of deployment. As in the 24 hour DOC sampling (Fig 3A), each optical property is generally inversely related to water depth in the main channel.

Fig 4.

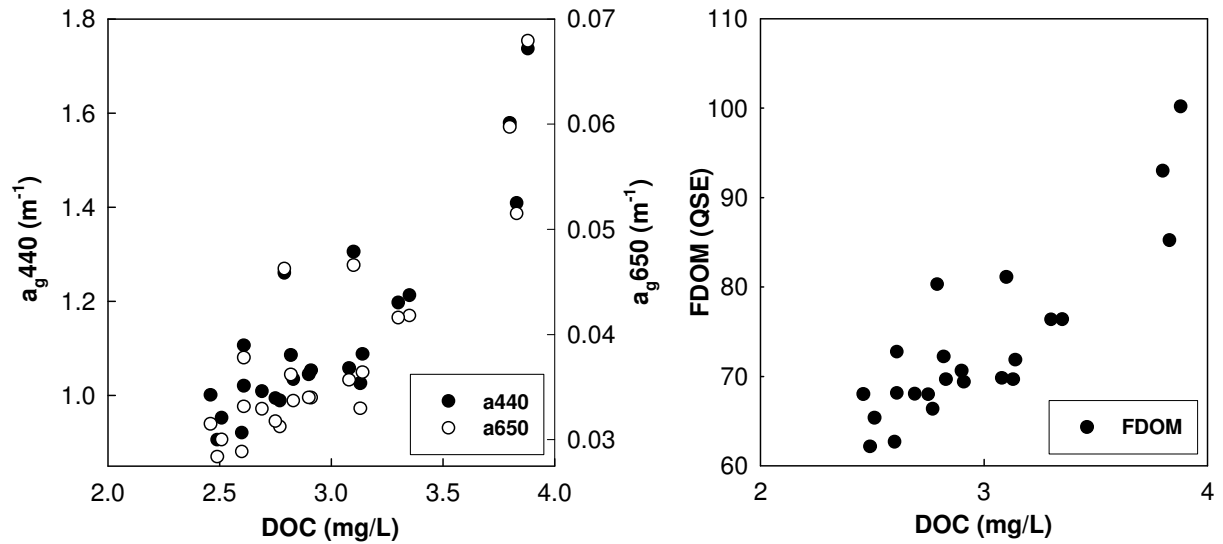


Figure 4. Dissolved organic carbon (DOC) concentrations measured from discrete samples, and optical properties measured in situ. In the left panel, a_{g440} and a_{g650} from the ac-9 correlate well with DOC ($R^2 = 0.76, 0.75$). In the right panel correlation of FDOM (WETStar CDOM fluorometer) to DOC is shown with $R^2 = 0.74$.

Fig 5.

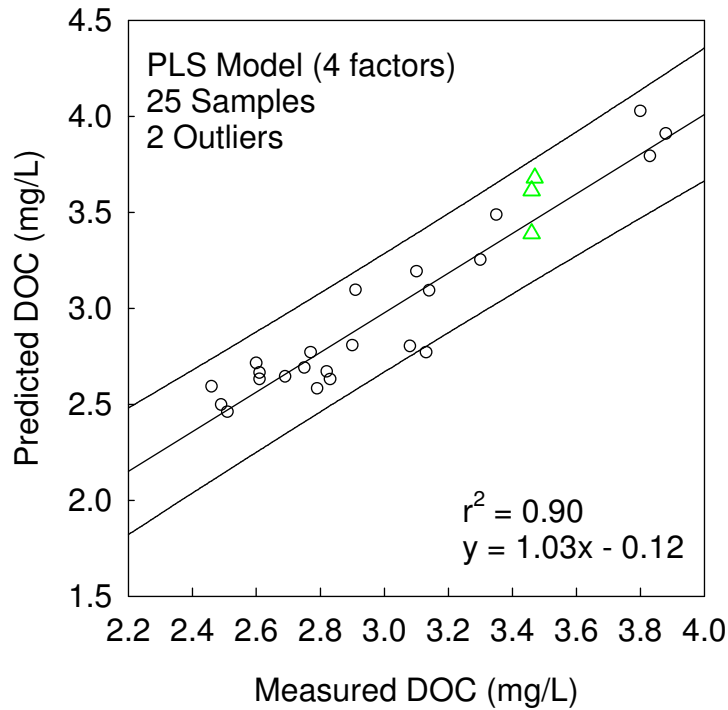


Figure 5. Measured DOC versus predicted DOC from the partial least squares regression model. Triangles show measured DOC values for samples collected before (Jan. 19, 2006) the 24 hour sampling period (Jan 31 – Feb 1). The individually collected samples were not used to construct the regression model and were used to validate the modeled DOC. The 1:1 regression line is shown, along with 95% prediction intervals on each side of the regression line.

Fig 6.

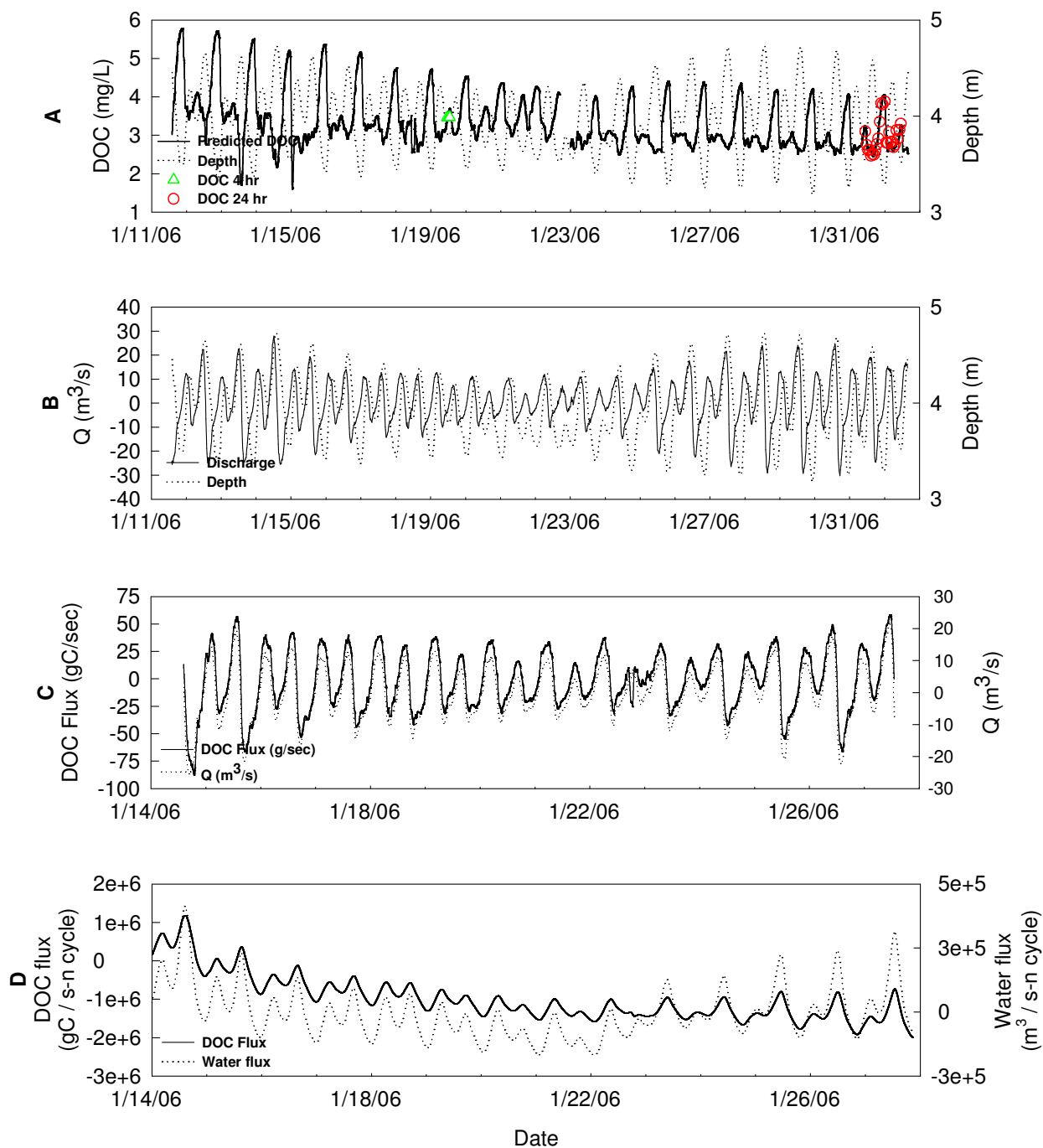


Figure 6 (A-D): Panel A, Modeled DOC time series and measured DOC (28 discrete samples). The PLS predictive model results for 25 discrete sample values shown as red circles. The discrete sample values shown as green triangles validate model performance. Panel B, Instantaneous discharge (Q) and water depth in the Browns Island main channel during the entire deployment. Negative discharge values indicate ebb tides or off island direction, while positive indicate flood tides or on island direction. Panel C,

1
2
3 Instantaneous discharge (Q) and modeled DOC flux. The sign of the discharge relates to
4 the tidal cycle, where flood (positive) signifies on island direction and ebb (negative)
5 signifies off island direction. Panel D, The cumulative spring–neap DOC flux and water
6 flux (integrated over 14.7 days starting from 1/14/06). Note that in the beginning of the
7 time series, as the tide is transitioning from spring to neap, there is a transition from on-
8 island (positive) DOC flux to an off-island (negative) flux.
9
10
11
12
13
14
15
16
17
18
19
20
21
22
23
24
25
26
27
28
29
30
31
32
33
34
35
36
37
38
39
40
41
42
43
44
45
46
47
48
49
50
51
52
53
54
55
56
57
58
59
60

For Review Only

Fig 7.

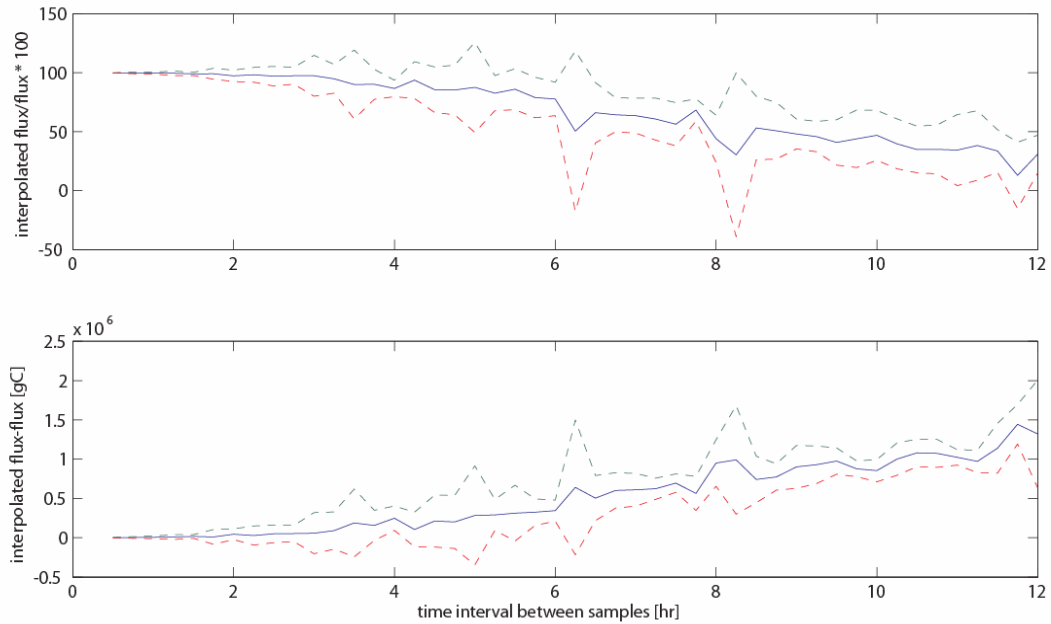


Figure 7: Fig 7A—Ratio of interpolated spring–neap DOC flux at indicated interval to DOC flux calculated using a 0.5 hr sampling interval. Fig 7B—Difference between interpolated spring–neap DOC flux at indicated interval and the DOC flux calculated using a 0.5 hr sampling interval. Solid blue lines denote the mean over 22 spring–neap tide realizations; dashed lines denote \pm one standard deviation around the mean.

Fig 8.

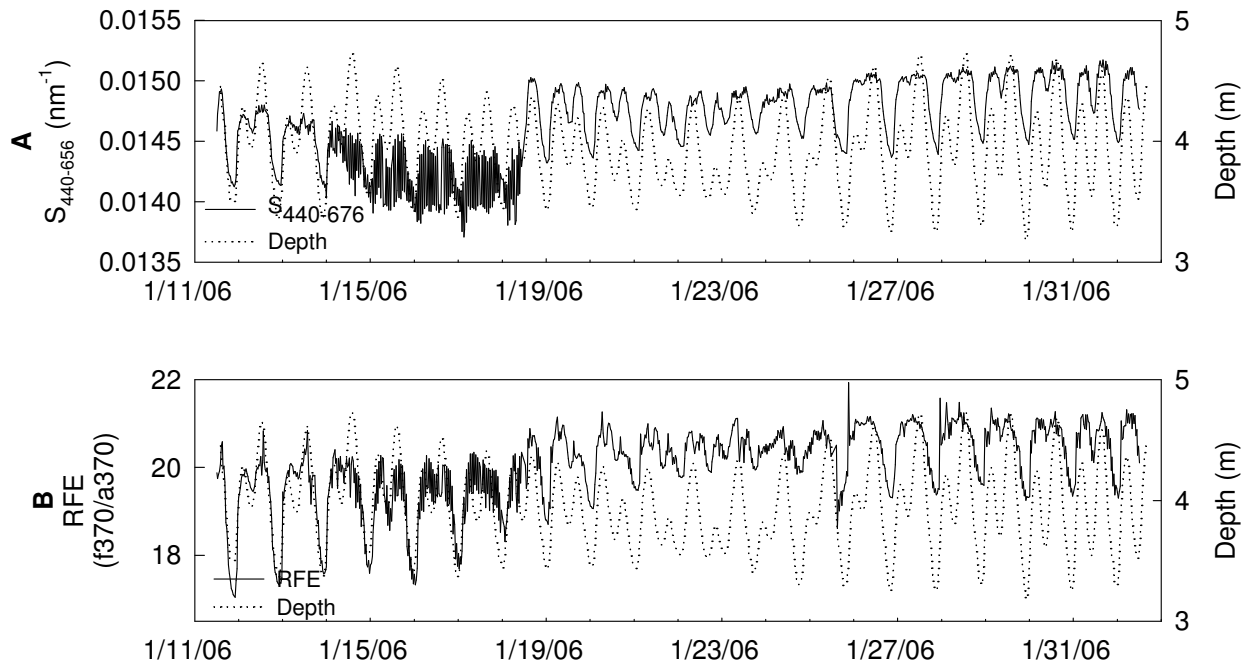


Figure 8. Fig 8A—Time series of CDOM spectral slope (S) and water depth in the main channel over the deployment period. Fig 8B—Time series of the relative fluorescence efficiency (RFE) and water depth. Variations in the slope of RFE are consistent with changes in spectral slope at tidal scales. Changes in signal character at times of instrument servicing (~ 4 hours on 1/18 and 1/25) reveal the sensitivity of its value to biofouling.